*Skin Research and Technology 2004; **10**: 161–168*
Printed in Denmark. All rights reserved

Skin Research and Technology

Pilot study of dermal and subcutaneous fat structures by MRI in individuals who differ in gender, BMI, and cellulite grading

F. Mirrashed[1], J. C. Sharp[1], V. Krause[1], J. Morgan[2] and B. Tomanek[1]

[1]*Institute for Biodiagnostics, National Research Council Canada, Winnipeg, Canada and* [2]*The Procter & Gamble Company, Cincinnati, OH, USA*

Background/aims: Puckered, dimply skin on the thighs, hips, and buttocks is known as cellulite. The cause of cellulite is not known, although there are a number of different hypotheses. In this study, we use magnetic resonance (MR) micro-imaging to study cellulite skin. To the best of our knowledge, this is the first reported MR study of cellulite.

Methods: High-resolution *in vivo* MR images of the post-lateral thigh skin of two male groups and four female groups were obtained. Subjects were grouped according to their body mass index (BMI) and cellulite grade. A qualitative assessment of how MRI can be used to differentiate skin tissue at different levels of cellulite grading was performed.

Results: We found that changes in skin architecture with cellulite can be visualized by *in vivo* MR micro-imaging. The skin fat layers beneath the dermis and down to the level of muscles are well visualized in the images. Also, the diffuse pattern of extrusion of underlying adipose tissue into dermis is clearly imaged, and was found to correlate with cellulite grading.We also show that other skin tissue parameters such as (a) the percentile of adipose vs. connective tissue in a given volume of hypodermis and (b) the percentile of hypodermic invaginations inside the dermis are correlated with cellulite grade.

Conclusion: MR images can be interpreted to measure tissue parameters correlated with cellulite. Considering that we had only three subjects in each group, the achievements of this pilot study were highly satisfactory. We have shown that the *in vivo* micro-MR is a technique able to detect the effects of cellulite and gender. This study can be extended for further investigations of drugs and/or medical devices for cellulite treatment.

Key words: cellulite – skin-imaging – micro-MRI – surface coil – dermis-hypodermis interface – skin atrophy

Accepted for publication 30 January 2004

Figure 1 SHOWS a schematic diagram of the skin structure divided into five zones. The gray layer at the surface of the skin represents the epidermis. Layer 1 represents coarse fibrous corium. Layer 2 represents small papillae adiposae, which break up into the corium and surround hair bulbs, sweat glands, and blood vessels, and protect them against pressure and shearing forces. These and the standing fat cell from underneath can change shape under pressure (whereas the volume remains constant) and hence change the appearance of the skin surface. Subcutaneous tissue is composed of three layers of fat (Zones 3–5 in Fig. 1) with two planes of connective tissue between them. Zone 3 is the upper zone of subcutis with standing fat-cell chambers and radially running septa of connective tissue. Zone 4 is the middle zone of the subcutis layer with squat fat chambers and septa of connective tissue that runs tangential to the fascia (a linear connective tissue connects the deep fat layer of the skin to muscle). The subdermal connective tissues exist as thin vertical streaks (fibrous septa), which connect the deep dermis to fascia concurrent with fat lobules. Zone 5 in Fig. 1 is the lower zone of subcutis.

What causes cellulite? Some of the different hypotheses involve: weak, abnormally shaped, less flexible connective tissue, tending to pull

This work was presented (oral) in International Society for Magnetic Resonance in Medicine (ISMRM) in Toronto, Canada in 2003.

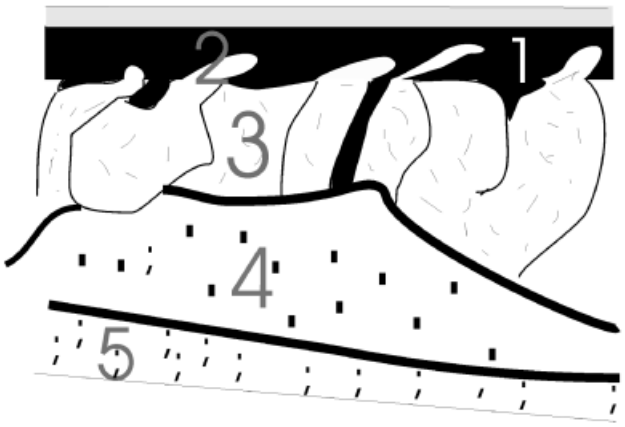

Fig. 1. A schematic diagram of skin structure showing five zones. The gray layer is the surface of the skin called epidermis. Zone 1 is the dermis. Zone 2 is the extrusion of the hypodermis into the dermis. Zones 3–5 are the upper, middle, and lower parts of the hypodermis.

down on the surface of the skin; lipodystrophy ('misshapen fat') in one or several specific areas pushed toward skin surface; circulation disorders; hormonal factors; and hereditary factors (sex, race, biotype, etc.) (1–10).

Skin imaging

Currently high-resolution ultrasound is a common technique for *in vivo* cellulite imaging. With ultrasound techniques, pulses of ultrasound waves are emitted into the skin. The cross section of the skin can be imaged by detecting reflected acoustic waves, which occur from transitions between tissue layers with different acoustic impedance. Using ultrasound, Lucassen et al. (11) focused on imaging the dermis–hypodermis tissue interface to measure the roughness of the upper layer of fat cells and used this factor to assess the effect of the treatment; however, this technique did not allow them to study the effect of cellulite on the skin structure. Ultrasound imaging provides information about the connective tissue of the dermal layer and the irregularity of the surface between the dermis and hypodermis, but cannot visualize adipose tissue and hence cannot provide information on histopathology of the fat lobules. In this study, we aim to assess the affected skin with cellulite. Hence we have to observe and quantify the changes in cellulite skin layers compared with unaffected skin. High-resolution *in vivo* magnetic resonance (MR) micro-imaging can visualize the architecture of the skin layers in the dermis and hypodermis without being subjected to operator error as is the case with ultrasound technique. Micro-MRI can clearly show the thickness and the structural alterations of the connective tissue in the dermis and the subcutaneous fat cells in the hypodermis correlated with abnormalities of the skin. Also, MRI has the advantage of acquiring coronal images. The coronal slice orientation cuts perpendicularly through the streaks of the connective tissues that run below the dermis into the hypodermis. High-resolution coronal slices allow for quantitative analysis of connective tissue vs. adipose tissue. Unfortunately, clinical high field MRI systems capable of high-resolution imaging are not yet readily available, whereas the necessary ultrasound equipment is readily available.

In this study, using micro-imaging MRI we imaged the skin of the lateral aspect of the thigh in groups of human subjects with different body mass index (BMI) and cellulite grading. We conducted a quantitative analysis of the obtained images and demonstrate that the changes in skin architecture and the cellulite grading are correlated.

Materials and Methods

Imaging was carried out using a 3 T whole-body MRI magnet (Magnex, Oxfordshire, UK) with an SMIS console (SMIS, England). The radio-frequency (RF) coil was a single ring surface coil inductively coupled with a matching ring. The radius of the coil used was selected (4 and 6 cm) for each individual depending on the thickness of the contour of fat surrounding the body. For subjects with a thick fat layer, the bigger coil was used allow deeper tissues to be imaged. The study was conducted in compliance with the institution's Research Ethics Board (REB), and informed consent was obtained from all subjects.

The postlateral thigh skin of six men and 12 women were imaged. All subjects were within the age range of 18–46 years. Subjects were categorized by their BMI and cellulite grading. In this study, BMI between 18 and 25 was defined as low BMI, with BMI 30 above defined as high. The study consisted of two male groups and four female groups (three in each group). The males, all classified as low cellulite grade were simply divided into low and high BMI groups. The females were divided into low and high cellulite categories, then further into low and high BMI groups, making four female groups in all. Low

TABLE 1. Visual cellulite grading scale

Cellulite grading scale	Skin appearance
0	No dimpling – smooth skin
1	Few number of small, shallow, visible dimples, sparsely located on the thighs
2	Moderate number of visible dimples (some large) on the thighs
3	Large number of visible dimples (many large) over most of the thighs
4	Cottage cheese appearance of skin

Whole units reflect generalized condition. Half units may be used to represent intermediate conditions.

cellulite was defined as $(0,\ldots,0.5)$ and high cellulite as $(2,\ldots,4)$. Cellulite grading was performed by expert inspection according to a visual cellulite grading scale (see Table 1). The cellulite scale varies from Grade 0 (smooth skin) to Grade 4 ('cottage cheese' appearance). Thirty-five millimeter photos were taken of posterolateral thigh skin for each subject, seated with the affected leg flexed to 90° at the hip and knee.

Patient setup

Patients were positioned supine in the magnet bore, feet first. The examined thigh was placed with its dorsal surface against the RF coil on a support platform. The coil was strapped to the thigh 10–15 cm below the buttocks. To prevent motion artifacts, the limb and knee were immobilized by using straps. To make sure that the affected area was imaged, the presence of cellulite was defined as evidence of dimpling of the skin of the poster–lateral thigh when the subject sits with the affected leg flexed to 90° at the hip and knee. Areas containing dimples are designated as 'affected' and any continuous area at least 3 cm in diameter in which no dimpling is evident is designated as 'unaffected'. The skin under examination was positioned against the middle of the ring of the coil. A picture of a coil installed on the patient bed is shown in Fig. 2.

Experimental design

Four MR data sets were collected for each subject. We obtained axial and sagittal multi-slice gradient echo (GE) T1-weighted images with TR = 340 ms, TE = 19 ms, field of view (FOV) 40 mm × 40 mm, imaging matrix 256 × 256. The in-plane resolution was less than 160 μm, slice thickness 1 mm, and imaging time less than 10 min for each set. An axial anatomical GE

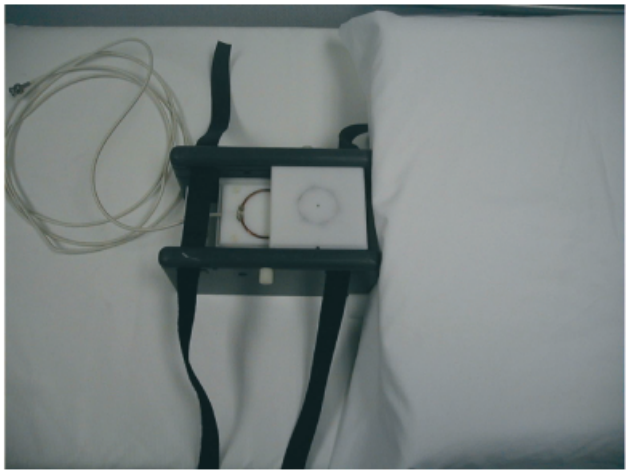

Fig. 2. The RF coil installed on the patient bed. The coil is fixed tuned, with a matching ring moveable by the knob at the side.

image with FOV = 70 mm × 70 mm was taken to visualize the skin layers and muscle for reference and was not used in data processing.

We also acquired a set of coronal GE images, TR = 1215 ms, TE = 26 ms, FOV 75 mm × 75 mm, matrix 512 × 512 with in-plane resolution less than 150 μm, and slice thickness 1 mm. Coronal slice orientation cuts perpendicularly through the streaks of the connective tissues that run below the dermis into the hypodermis (see Fig. 1), allowing quantitative analysis of connective tissue vs. adipose tissue. Since the slice thickness is 1 mm, we assume that partial volume effects are minor and that our quantitative assessment is reliable. Using 'Marevisi', our in-house image analysis program, a quantitative analysis was applied to each set of images. From the sagittal images, the thickness of the dermis, hypodermis and the percent of fat inclusion into the dermis were measured for each subject. Using the coronal slices, the percent of fat and connective tissue in hypodermis were asssessed for each subject.

Method of image processing

Using the same software program, we classified pixels as either fat or connective tissue by applying threshold levels to the MR images. We make the assumption that within the hypodermis and/or dermis, there are only two MR-distunguishable compartments, namely, fat (i.e. bright pixels) and fibrous tissue (i.e. low intensity pixels). To be able to cover most of the hypodermis, we analyzed three sucessive 1 mm coronal slices through the hypoderims (parallel to the skin surface).

Slice 1 was located just at the border of dermal–adipose layer with the second and third progressively located deep in the hypodermis. We analyzed the data in each slice for area fraction of fibrous vs. fat tissue.

The percentage of fat and fibrous tissue in the hypodermis and dermis was calculated as follows. Firstly, the maximum pixel intensity within a region identified as 100% fibrous tissue was obtained. Secondly, the minimum pixel intensity within a region identified as 100% fat was obtained. Finally, the threshold was calculated as the intensity average of these two reference intensities. From the number of pixels below and above the threshold for each slice the percentile area of the fibrous tissue and fat were measured, respectively.

Note

Sagittal and axial slice orientations (i.e. perpendicular to the surface of the skin) show the fat inclusion into the dermis from the hypodermis. The percent of fat (i.e. high intensity pixels) vs. fibrous tissue (i.e. dark intensity pixels) was measured in the dermis. There is also another type of high-intensity pixel from the hypodermis into the dermis in continuity with the epidermis, which corresponds to pilosebaceous units. Because the epidermis is very thin in thigh skin, it was hard to distinguish and exclude the pilosebaceous units from the hypodermic invagination in the dermis. We assumed that the sebaceous units have similar density in the individual regardless of their cellulite grading, hence the effect of pilosebaceous units on the measurements is negligible.

Statistics

Comparison of data between the groups was carried out by analysis of variance using one-way ANOVA to detect an overall difference between the three groups, where differences were considered significant at $P \leq 0.05$. We also used Duncan's multiple range test, to detect differences between groups, where differences were considered significant at $P \leq 0.05$.

Results

To show the appearance of cellulite skin, examples of 35 mm photos of posterolateral thigh skin from subjects with different cellulite grading is shown in Fig. 3. Good quality high-resolution GE images were obtained. The resolution and quality of the images are sufficient to observe clearly the skin structure at all layers. For all images shown in this work, the display orientation of skin surface toward deeper tissue is from right to left. A typical MRI image of thigh skin is shown in Fig. 4. In this image, the skin structure shown by MRI is explained using the same definitions as we used in the schematic diagram in Fig. 1. Beneath the superficial thin bright layer (epidermis) is the dark dermis layer (Zone 1). Below the dermis is the bright layer called the hypodermis, which is divided into Zones 3–5. Muscle is shown as a semi-dark tissue beneath the hypodermis. Zone 2 shows the inclusion of fat from the hypodermis into the dermis. Similar to the Fig. 4 example, all sagittal- and axial-oriented images clearly showed the thickness of the hypodermis and dermis; the extrusion pattern of hypodermic tissue inside the dermis; dark septated structure separating fat lobules inside hypodermis; anteroposterior dimension of fat lobules; and septa thickness.

High BMI group

MRI results are tabulated in Table 2. The dermis is significantly thinner in women than in men

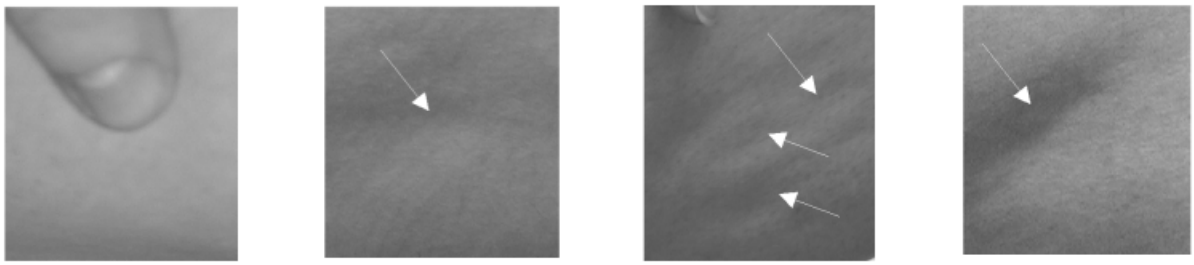

Fig. 3. Thirty-five millimeter photo of posterolateral thigh skin from subjects with different cellulite grading. From left to right the cellulite grading is 0, 0.5, 1.5, and 3.

($P<0.05$). Among women, the dermis in the affected skin is thinner compared with unaffected skin ($P=0.09$).

The percentile of fat inclusion into the dermis is found to be significantly ($P<0.05$) higher in females with high cellulite compared with men and low cellulite females. Figure 5 shows examples of sagittal images of normal skin (i.e. cellulite grade = 0) of men (a, b) and women (c, d); all subjects are from high BMI groups. These images (a, b) clearly show that the fibrous septa are thicker in males compared with females and are arranged in planes oblique in smaller capsules, hence fat lobules are smaller. In women, the septa are more radial and fat lobules are in larger dimension (c, d). With respect to the thickness of fat layer of the skin, our measurements show that there is no significant difference among the subjects in the high BMI group. Figure 6a–c shows the coronal slice orientation of a male skin in the high BMI group. Slice (a) is acquired at the region of the junction between the dermis and adipose layer. Slice (b) is obtained from 1 mm immediately below the junction of the dermis and hypodermis. Slice (c) is acquired from a region within the hypodermis. The percentile of the adipose vs. connective tissue in each one of slices a-c was assessed for all the subjects in the high BMI group. No differences were found between males and females with low cellulite. Women with high cellulite showed a significant ($P<0.05$) decrease in the percentile of fibrous tissue in every one of the slices a–c compared with men.

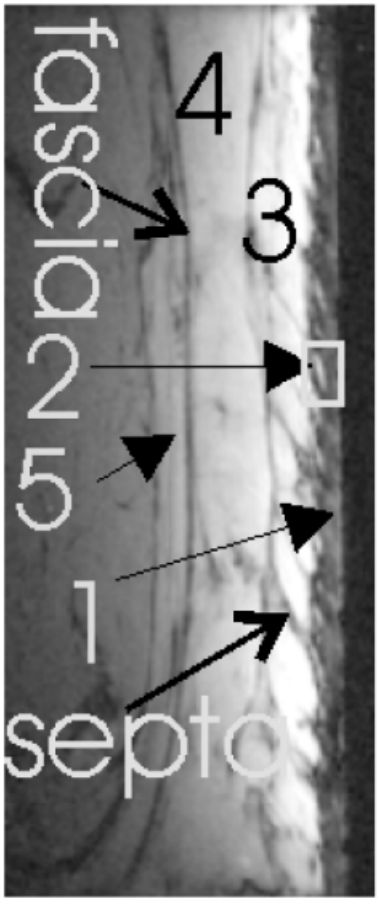

Fig. 4. Typical MRI thigh skin. Right to left is the surface of the skin to muscle with a plane resolution of 273 × 273 μm. From right to left is the surface of the skin, Zone 1 is the dermis layer, and Zone 2 is the bright pixels shown in the box extrusion of hypodermic tissue inside the dermis. Zones 3–5 are the upper, middle, and lower parts of the hypodermis. Dark fibrous streaks separating fat lobules inside the hypodermis (fibrous septa) and fascia; the linear connective tissue connecting the deep fat layer of the skin to muscle is clearly visible in the image.

Low BMI group

MRI results are tabulated in Table 3. The thickness of the hypodermis in men and women in all our subjects at low BMI group was assessed. Compared with women with unaffected skin, the hypodermis in women with high cellulite is thicker ($P<0.07$), whereas in men the hypodermis is significantly thinner ($P<0.05$). Figure 7 compares the skin of two females both having the same BMI = 25. Fig. 7a shows cellulite grade 2.5,

TABLE 2. MRI results for high BMI groups

Measured parameter	High BMI Cellulite score = 0 Male ($n=3$)	High BMI Cellulite score = 2.5 Female ($n=3$)	High BMI Cellulite score = 0.17 Female ($n=3$) (control)
Thickness of the dermis	High ($P=0.09$)	Low ($P=0.09$)	1
Thickness of the hypodermis	–	–	1
% of fat inclusion into the dermis	–	High	1
% of fibrous tissue at the border of the dermal–adipose layer	–	Low	1
% of fibrous tissue 1mm immediately below the dermis	–	Low ($P=0.06$)	1
% of fibrous tissue inside the hypodermis	–	Low	1

In this table, 'Low' means significantly lower; 'High' means significantly higher; and '–' means no significant difference compared to control ($P<0.05$, unless mentioned otherwise). The cellulite score shown for each column is the average score for the group.

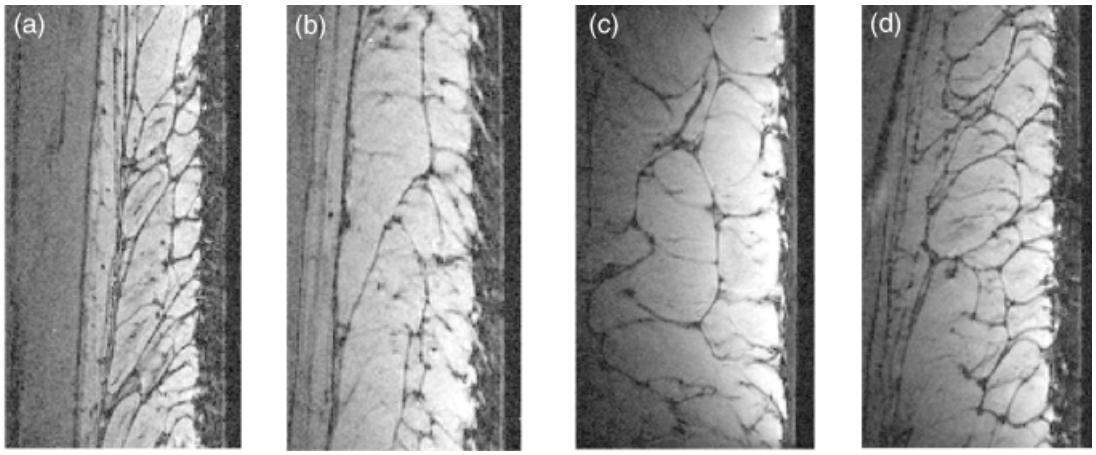

Fig. 5. Examples of sagittal images of normal skin (i.e. cellulite grade = 0) of men (a, b) and women (c, d), all subjects are from the high BMI group.

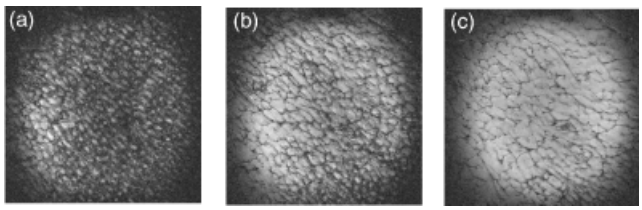

Fig. 6. Coronal slice orientation, 147 μm × 147 μm in-plane resolution, of a 1 mm thick slice of male normal skin. Slice (a) is acquired at the junction of the dermis and adipose layer. Slice (b) is obtained from 1 mm immediately below the junction of the dermis and hypodermis. Slice (c) is acquired from a region within the hypodermis.

with 16.2 mm hypodermal thickness, whereas Fig. 7b shows unaffected skin with an 11.3 mm thickness. It is also shown in these images that the subcutaneous adipose tissue lobules are larger in the skin with high cellulite compared with unaffected skin.

Discussion

General

We have successfully shown that *in vivo* MR micro-imaging can visualize changes in skin architecture associated with cellulite. In this study, the structural alterations of the skin correlated with cellulite grade were measured by assessment of the thickness of the hypodermis (subcutaneous fat), thickness of the dermis (connective tissue), the percentage of hypodermic invaginations inside the dermis, and the percentage of adipose vs. connective tissue in a given volume of the hypodermis.

The density of connective tissue within the skin fat structure was assessed quantitatively by measuring signal void pixels per unit volume within the hypodermis. Also, the bright pixels per unit volume inside the dermis as an index of the density of hypodermis invagination into the dermis were measured. Both factors were found to be correlated to cellulite grading.

Gender

Our MRI results support the observed difference in cellulite grading between the genders. Compared with men, in women because the upper part of the subcutaneous tissue is thicker and the

TABLE 3. MRI results for the low BMI group

Measured parameter	Low BMI Cellulite score = 0 Male ($n = 3$)	Low BMI Cellulite score = 2.25 Female ($n = 2$)	Low BMI Cellulite score = 0 Female ($n = 3$) (control)
Thickness of the dermis	–	–	1
Thickness of the hypodermis	Low	High ($P = 0.07$)	1
% of fat inclusion into the dermis	–	–	1
% of fibrous tissue at the border of the dermal–adipose layer	–	–	1
% of fibrous tissue 1mm immediately below the dermis	–	–	1
% of fibrous tissue inside the hypodermis	–	–	1

In this table, 'Low' means significantly lower; 'High' means significantly higher; and '–' means no significant difference compared to control ($P < 0.05$, unless mentioned otherwise). The cellulite score shown for each column is the average score for the group.

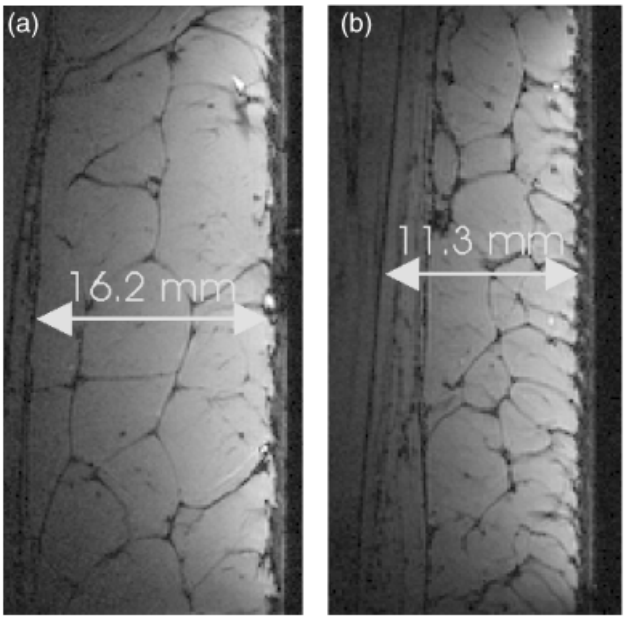

Fig. 7. Skin of two females both from low BMI group: (a) cellulite grade = 2.5, hypodermis 16.2 mm; and (b) cellulite grade = 0.0, hypodermis 11.3 mm.

fat cell chambers are bigger and radial (Fig. 5c, d), the compression and bulging of the upper fat cell chamber system might cause the overlying skin to protrude and produce deformation and pits (i.e. the mattress phenomenon of cellulite). In the comparable skin of thighs of men (Fig. 5a, b), the adipose tissue is thinner and has a network of thicker oblique criss-crossing septa of connective tissue that divide the fat cell chambers into small, polygonal units. This strong network of connective tissue in the fat layer and thicker dermis in male skin compared with female skin may prevent the papillae adiposae from protruding upon the overlying cutis. This might explain why cellulite affects 90% of all women, but few men.

High BMI

From the results derived from high BMIs image analysis it is likely that for this group their susceptibility to cellulite is determined by the weak and less dense connective tissue structure. In this group (a) the number of septa (i.e. connective tissue formed by the elastic and predominantly collagen fibers) between adipose tissue lobules is significantly lower in the all slices cut through hypodermis; (b) the amount of extrusion of adipose tissue into the dermis is significantly higher; and (c) and the dermis is significantly thinner compared with unaffected skin.

Low BMI

The MRI results for low BMI subjects suggest that cellulite – where it occurs – is likely to be the result of differences in adipose tissue, since so far MRI noted a significant increase in fat layer thickness and larger subcutaneous adipose tissue lobules. Lack of sufficient data points in the low BMI groups is an alternative explanation for the absence of any observed differences between normal and cellulite skin, except for hypodermal thickness. The percentile of fat inclusion into the dermis was not assessed for low BMI groups because in this group the skin layers of fat and dermis are very thin – hence the identification of the regions with 100% fat or 100% connective tissue inside the dermis was difficult.

If a thicker fat layer makes skin more susceptible to cellulite, then this may be a reason why women with low BMI are less likely to be affected by cellulite.

This was a pilot study, with three subjects in each category, where statistical considerations suggest that a minimum of nine subjects in each group would be better able to derive a strong conclusion. Nevertheless, we successfully managed to obtain interesting results from this study, which is promising for further investigations. From this study, we found that MRI microscopy of cellulite is a potential tool for further investigation for drug and or medical device test for cellulite treatment.

Acknowledgment

We thank Dr R. Summers for his helpful discussion in statistics.

References

1. Rossi AB, Vergnanini AL. Cellulite: a review. J Eur Acad Dermatol Venereol 2000 Jul; 14: 251–262 (review).
2. Pierard G, Nizet, Pierard F. Cellulite: from standing fat herniation to hypodermal stretch marks. Am J Dermatol 2000 Feb; 22: 34–37.
3. Collis, Elliot, Sharpe C, Sharpe DT. cellulite treatment: a myth or reality: a prospective random. Plast Reconstr Surg 1999 Sep; 104: 1110–1114.
4. Rosenbaum M, Prieto V, Hellmer J, Boschmann M, Krueger J, Leibel RL, Ship AG. An exploratory investigation of the morphology and biochemistry of cellulite. Plast Reconstr Surg 1998 Jun; 101: 1934–1939.
5. Draelos M. Cellulite. Etiology and purported treatment. Dermatol Surg 1997 Dec; 23: 1177–1178.
6. Dickinson G-H. Aminophylline for cellulite removal. Ann Pharmacother 1996 Mar; 30: 292–293.

7. Lotti T, Ghersetich I, Grappone C, Dini G. Proteoglycans in so-called cellulite. Int J Dermatol 1990 May; 29: 272–274.
8. Nurnberger F, Muller G. So-called cellulite: an invented disease. J Dermatol Surg Oncol 1978 Mar; 4: 221–229.
9. Scherwitz B-F. So-called cellulite. J Dermatol Surg Oncol 1978 Mar; 4: 230–234.
10. Quaglino Jr. D, Bergamini G, Boraldi F, Pasquali Ronchetti I. Ultrastructural and morphometrical evaluation on normal human dermal connective tissue – the influence of age, sex and body region. Brit J Dermatol 1996; 134: 1013–1022.
11. Lucassen GW, Van der Sluys WLN, Van herk JJ, Nuijs AM, Wierenga PE, Barej AO, Lambrecht R. The effectiveness of massage treatment on cellulite as monitored by ultrasound imaging. Skin Res Technol 1997; 3: 154–160.

Address:
F. Mirrashed
NRC - 1BD
Institute of Biodiagnostics
435 Ellice Ave,
Winnipeg, MB
Canada R3B 1YB

Tel: +1-204-984 7036
Fax: +1-204-984 6321
e-mail: fmirrashed@ottawahospital.on.ca